International Journal of Scientific Engineering and Research (IJSER)
ISSN (Online): 2347-3878
Impact Factor (2020): 6.733

Numerical Investigation of Oil Production Enhancement using Controlled Salinity and Enzyme Injection Process

Udo W. Udoma[1], Tinuola Udoh[2]

[1, 2]Chemical/Petrochemical Engineering, Faculty of Engineering, AkwaIbom State University, MkpatEnin, AkwaIbom State. Nigeria

[1]Correspondence: *udoudoma20[at]gmail.com*
Tel.: +2348080200820

Abstract: ***In this work, a simple two-phase flow model based on Buckley Leverette theory was developed and the model was validated using the analytical solution of the equation. The model was then upgraded to implement water flooding operation using a previous work as a case study. Finally, the model was applied to an experimental enhanced oil recovery process that was previously carried out to establish that it can be applied in real life situations. The result from the model showed a good agreement with the result of the experimental work.***

Keywords: enhanced oil recovery, modeling, two-phase flow, Buckley Leverette equation

1. Introduction

Petroleum production from oil reservoirs involves three distinct phases namely primary, secondary and tertiary (or enhanced) recovery. During the primary oil recovery, the natural pressure of the reservoir drive oil into the bored well from where the oil is brought to the surface (Petal *et al.,* 2015; Zeng, 2021). The secondary recovery usually involves water flooding and/or gas flooding. Typically, two thirds of the original oil in place (OOIP) in a reservoir is not produced by primary and secondary oil recovery methods and is still pending for recovery by efficient enhanced oil recovery methods **(**Tunio *et al.,* 2011; Mandal 2015; Petal *et al.,* 2015; Keshtkar *et al*., 2016). Reservoir rock and fluid properties must be well studied and understood if maximum oil recovery is to be obtained from the oil reservoir.

Rock properties are determined by performing laboratory analyses on cores from the reservoirs. The properties normally evaluated include porosity, permeability, saturation, capillary pressure, relative permeability, wettability, surface and Interfacial tension, etc., (Ahmed 2006; Alfazazi *et al*., 2019; Gbadamosi *et al.,* 2019).

Previous studies have demonstrated the enhanced oil recovery (EOR) potential of controlled salinity and enzyme process. The use of enzyme aids the recovery of oil by lowering the interfacial tension between oil and brine and altering the wettability on rock grains to a more water-wet condition. (Nazir*iet al*., 2009;Khusainova, 2016). Rahayyem*et al*., (2019) carried out an experimental study using micro scale approach to investigate the effect of enzyme enhanced oil recovery andmore oil recovery was observed with the use of the enzyme.

Also, Udoh and Vinogradov (2021) compared the result of controlled salinity brine to controlled salinity brine with biosurfactants(greenzyme and rhamnolipids) during a core flooding experiments. The results further confirm a greater oil recovery when enzyme was introduced during the process. Although some experimental work had been done on combined controlled salinity enzyme enhanced oil recovery, the mechanisms involved in the process have not been fully unraveled due to the complexity of the processes involved. More so, experimental works are very expensive and time consuming. There is therefore a need for numerical modelling of the process which will ameliorate these challenges. A proper modelling of the process will help in the interpretation and understanding of the recovery mechanisms and to obtain relevant parameters which may be used in subsequent enhanced oil recovery (EOR) process at laboratory and reservoir scales.

The aim of this work is to develop a numerical model to simulate a controlled salinity enzyme enhanced oil recovery process at a laboratory scale otherwise known as core flooding process. Numerical modeling translates problem from an application area into mathematical formulations whose theoretical and numerical analysis provides insight, answers, and guidance useful for the originating application (Neumaier, 2004). The core flooding numerical modeling consists of a set of differential equations that describe the flow of fluids together with an appropriate set of boundaries and/or initial conditions. Solving these equations with the use of the boundary conditions will help to describe the fluid flow inside a porous rock system.

2. Methodology

The continuity and momentum equations were used to describe the two phase-flow in a porous medium for each phase. In writing the equations for fluid flows, several quantities peculiar to multiphase flow, such as saturation, capillary pressure and relative permeability were introduced. To obtain the analytical solution to the equations, a one-dimensional model with homogeneous rock properties was considered. The temperature was constant, the fluids were biphasic and incompressible, and the capillary pressure as well as gravity were ignored. When there is no mass transfer between phases in the immiscible flow, mass is conserved

Licensed Under Creative Commons Attribution CC BY

within each phase, Mass conservation (Continuity) equation for each phase (α) is given as:

$$\frac{\partial(\phi S_\alpha \rho_\alpha)}{\partial t} + \nabla.(\rho_\alpha u_\alpha) = q_\alpha, \qquad \alpha = o, w, \qquad (1)$$

where $\phi$is the porosity of the porous medium and $s_{\alpha,}\ \rho_{\alpha,}\ u_{\alpha,\ and}\ q_\alpha$ are the saturation, density, Darcy velocity and mass flow rate respectively. The Darcy velocity for each phase is defined as

$$u_\alpha = -\frac{kk_{r\alpha}}{\mu_\alpha}(\nabla p_\alpha - p_\alpha g \nabla z), \qquad (2)$$

whereμ_α is dynamic viscosity, k is the absolute permeabilityof the porous medium, $k_{r\alpha}$ is the relative permeability, p_α is thepressure in each phase and gis the gravitational acceleration vector. As two fluids jointly filled the pores, the saturation is given as

$$s_w + s_o = 1, \qquad (3)$$

where$s_w$and $s_o$are the saturations of the water and oil phases, respectively.The pressure difference between the two phases was expressed in terms of the capillary pressure as stated in equation 4 where $p_o$is the pressure of oil and p_w is the pressure of water.

$$p_c = p_o - p_w. \qquad (4)$$

For two-phase flow, the velocity was expressed in terms of the total velocity (u) which is the sum of the oil and water velocities, expressed as

$$u = u_w + u_o \qquad (5)$$

For the incompressible fluids,

$$\nabla.u = q \qquad (6)$$

When the mass conservation equation was applied into momentum equation,

$$\frac{\partial(\phi s_\alpha \rho_\alpha)}{\partial t} + \nabla\left[\rho_\alpha\left(\frac{kk_\alpha}{\mu_\alpha}(\nabla p_\alpha - p_\alpha g \nabla z)\right)\right] = q_\alpha \quad (7)$$

Considering the assumptions as stated above,equation (1) is written for the two phase system as

$$\nabla.u = q_o + q_w \quad (8)$$

Subtracting continuity equation for the two phases produces

$$\phi\frac{\partial s_\alpha}{\partial t} + \nabla.u = q_\alpha \quad (9)$$

This leads to the total velocity as follows

$$u = -k[\lambda\nabla p - \lambda_w \nabla p_c - (\lambda_w \rho_w + \lambda_\alpha \rho_\alpha) g \nabla z] \quad (10)$$

When p_c was neglected in total velocities equation, then

$$u = -k[\lambda\nabla p - (\lambda_w \rho_w + \lambda_\alpha \rho_\alpha) g \nabla z] \quad (11)$$

For water and oil flowing in one directional homogeneous incompressible medium, the equation of flow was written as;

$$\left(\frac{dx}{dt}\right)_{sw} = \frac{-u}{A\phi}\left(\frac{df_w}{ds_w}\right)_{sw} \qquad (12)$$

where$u$ is the total flow rate, f_w is the fractional flow of water. This is the Buckley Leverette advanced equation. The Galerkin finite element procedure was used to perform the finite element discretization for Buckley Leveret problem (Arabzai and Honma, 2013). For water and oil flow in one directional homogeneous incompressible medium, the equation of flow was written as;

$$\frac{\partial}{\partial x}\left(K\lambda_w \frac{\partial p_w}{\partial x}\right) = \frac{\phi \partial S_w}{\partial t} \qquad (13)$$

$$\frac{\partial}{\partial x}\left(K\lambda_o \frac{\partial p_o}{\partial x}\right) = \frac{\phi \partial S_o}{\partial t} \qquad (14)$$

where,

$s_w + s_o = 1,$

$$p_c = p_o - p_w$$

Neglecting the capillary pressure, then $p_o\ and\ p_w$ was replaced by a single p

$$\frac{\partial}{\partial x}\left(K\lambda_w \frac{\partial p}{\partial x}\right) = \frac{\phi \partial S_w}{\partial t} \qquad (15)$$

$$\frac{\partial}{\partial x}\left(K\lambda_w \frac{\partial p}{\partial x}\right) = -\frac{\phi \partial S_o}{\partial t} \qquad (16)$$

By adding Equations (15) and (16), the equation of two-phase flow becomes

$$\frac{\partial}{\partial x}\left(K\lambda_w \frac{\partial p}{\partial x}\right) + \frac{\partial}{\partial x}\left(K\lambda_o \frac{\partial p}{\partial x}\right) = 0 \qquad (17)$$

This is the pressure equation in one directional flow. The boundary conditions are given as

$$-K\lambda_w \frac{\partial p}{\partial x} = \frac{\text{ut}}{A}\ at\ x = 0 \qquad (18)$$

$$\text{p=p at x=L} \qquad (19)$$

The Galerkin finite element procedure was used to perform the finite element discretisation for the Buckley Leveret problem. Applying Galerkin's criterion to Equation (17) leads to

$$\int_R = N_I\left\{\frac{\partial}{\partial x}\left(K\lambda_w \frac{\partial p}{\partial x}\right) + \frac{\partial}{\partial x}K\lambda_o \frac{\partial p}{\partial x}\right\}dR = 0 \quad (20)$$

whereN_I is the linearly independent weighing function. Applying the Green's theorem Equation (20) becomes

$$\int_R \frac{\partial N_I}{\partial x}\left(K\lambda_w \frac{\partial p}{\partial x} + K\lambda_o \frac{\partial p}{\partial x}\right)dR - \int_B N_I q dB = 0 \quad (21)$$

where$q$ is the outward normal finite on the boundary.

Introducing the following form of finite function

$$p(x,t) = N_J(x)P_J(t) \qquad (22)$$

and subdividing the region R into n finite elements, Equation (21) is written in matrix form as

$$\sum_{i=1}^{n}[E]^e\{P\}^{K+\frac{1}{2}} = \sum_{i=1}^{n}\{R\}^e \qquad (23)$$

where$K + \frac{1}{2}$ was the time step interval selected for the computation of P.

Licensed Under Creative Commons Attribution CC BY

Elements $[E]^e$ and $\{R\}^e$ were given by

$$\sum_{IJ}^{e} = \int_R k_x(\lambda_w + \lambda_o)\frac{\partial N_I}{\partial x}\frac{\partial N_j}{\partial x}\, dR \quad (24)$$

$$R^e = \int_{B^e} N_i\,[(q^{k+1} + q^k)/2]\, dB \quad (25)$$

Similarly, finite element formulation for Equation (17) was performed by applying Galerkin method.

$$\int_R N_I\left\{\frac{\partial}{\partial x}\left(K\lambda_w\frac{\partial p}{\partial x} - \emptyset\frac{\partial s_w}{\partial t}\right)\right\}dR = 0 \quad (26)$$

Applying the Green theorem, Equation (26) became

$$\int_R \frac{N_1}{\partial x}\left\{\frac{\partial}{\partial x}\left(K\lambda_w\frac{\partial p}{\partial x} - \emptyset\frac{\partial s_w}{\partial t}\right)\right\}dR = -\int_B N_I q dB + \left\{\frac{\partial}{\partial x}\left(N_I\emptyset\frac{\partial s_w}{\partial t}\right)\right\}dR \quad (27)$$

The trial functions
$p(x,t) = N_J(x)P_J\,(t)\ and\ s_w(x,t) = N_J(x)s_{w_J}\,(t)$were introduced and the region R was subdivided into n finite elements. Equation (27) was written in matrix form as

$$\sum_{i=1}^{n}[F]^e\{s_w\}^{K+1} = \sum_{i=1}^{n}\{U\}^e \quad (28)$$

In which the elements $[F]^e\ and\ \{U\}^e$were given by

$$[F]^e = \int_{R^e} N_i\frac{\phi}{\Delta t}N_I N_J dR \quad (29)$$

and

$$\{U\}^e = \left(\int_{R_e}\frac{\phi}{\Delta t}N_I N_J dR\right)\int_{wJ}^{k} - \left(\int_{R_e}k_x\lambda_w\right)\left(\frac{\partial N_I}{\partial x}\frac{\partial N_J}{\partial x}dR\right)p_J^{k+\frac{1}{2}} + \int_{B_e}N_I q^{k+\frac{1}{2}}dB \quad (30)$$

The appropriate solver was used to solve Equations (26) and (30) until successive changes of $p_J^{k+\frac{1}{2}}\ and\ s_w{}^{K+1}$were settled.

2.1 Buckley Leverette Simulation

The numerical flow model was first applied to Buckley Leverette problem in a homogenous medium with rock and fluid properties detailed in Table 1 and zero capillary. A one-dimensional 1 m core sample that was initially saturated with 100% oil was considered. At the commencement of the displacement process, water was continuously injected at constant rate into the core at one end to displace oil through the other end. The model was validated with known analytical solutions.

Table 1: Dataused for Buckley Leverette problem

Properties	Values	Units
Length(L)	1	m
Relative Permeability(k)	$1e^{-9}$	m^2
Porosity(ϕ)	50	%
Initial Water Saturation (s_{wi})	0	
Viscosity of water (μ_w)	0.001	Pa.s
Viscosity of oil (μ_0)	0.001	Pa.s
Injection rate (u_w)	0.001	m/s
Density of oil (ρ_0)	1000	kg/m^3
Density of oil (ρ_w)	1000	kg/m^3

2.2 Water Flooding Simulation

Thereafter, the model was used to simulate displacement process in which oil was displaced at constant pressure at the outlet. In this process, a core sample with 0.25 m length was considered and a constant water injection flow rate of $3.53e^{-6}\ m/s$ was used. The rock and fluid properties used for the simulation were adopted from the work of Diaz-Viera and Ortiz-Tapia (2015).

The details of the parameters used are presented in Table 2. The capillary pressure and the relative permeability to oil and water were determined based on Brooks and Corey model (Li and Horne, 2006; Szymkiewicz 2007; Diaz-Viera et al, 2008; Diaz-Viera and Ortiz-Tapia, 2015).

$$p_c = p_e(s_e)^{-1/\gamma} \quad (31)$$

where p_e is the entry capillary pressure and γ is the pore size distribution index and s_e is the effective or normalized wetting phase saturation.

$$k_{rw} = (s_e)^{\frac{2+3\gamma}{\gamma}} \quad (32)$$

$$k_{rnw} = (1-s_e)^2\left(1-(s_e)^{\frac{2+\gamma}{\gamma}}\right) \quad (33)$$

wheres_e is defined as

$$s_e = \frac{s_w - s_{wr}}{1 - s_{wr} - s_{nwr}} \quad (34)$$

The model was upgraded and used to simulate flow behaviour during secondary water flooding process at the laboratory scale.

Table 2: Data used for model upgrading

Properties	Values	Units
Length(L)	0.25	m
Porosity (ϕ)	22.95	%
Relative permeability(k)	326	mD
Residual water saturation	0.2	
Residual oil saturation	0.2	
Density of oil (ρ_0)	1000	kg/m^3
Density of water (ρ_w)	1000	kg/m^3
Viscosity of oil (μ_0	0.01	Pa.s
Viscosity of water (μ_w)	0.001	Pa.s
Injection rate	$3.53e^{-6}$	m/s
Pore size distribution (γ)	2	
Entry Capillary Pressure	10	KPa
Production pressure	10	MPa

2.3 Simulation of Experimental EOR Process

Following the successful application of the model to water flooding processes, the model was applied to experimental laboratory core flooding process. The case study considered in this work is the previous work by Udoh and Vinogradov (2021) in which a detailed experimental study was conducted on EOR applications of controlled salinity brine

Licensed Under Creative Commons Attribution CC BY

and biosurfactants (greenzyme and rhamnolipids). The model was used to simulate the experimental work with possibility of replicating the work and possibly carry out further investigations on the process.

Table 4: Data used for experimental simulation

Properties	CSB	CSBSB-R	CSBSB-G	units
Length(L)	0.076	0.076	0.076	m
Porosity(ϕ)	28	31	30	%
Relative permeability(k)	132	127	130	mD
Residual water saturation	0.39	0.41	0.43	
Density of water(ρ_w)	1000	1000	1000	kg/m^3
Density of oil (ρ_0)	906	906	906	kg/m^3
Viscosity of water(μ_w)	0.001	0.001	0.001	Pa.s
Viscosity of oil (μ_0)	0.006	0.006	0.006	Pa.s
Injection rate	1 and 3	1 and 3	1 and 3	ml/min
Pore size distribution (γ)	2	2	2	
Entry Capillary Pressure	10	10	10	KPa
Production pressure	10	10	10	MPa

3. Result and Discussion

The two-phase flow model based on Buckley Leverette theory was developed and the result of the model validation with the analytical solution of the equation is shown in Figure 1. The result of the developed model as implemented on secondary flooding process is also demonstrated. Finally, the upgrading and the application of the model to experimental enhanced oil recovery process is clearly presented.

3.1 Buckley Leverette Simulation Result

The result of the model developed reveals the displacement of oil by water. The solid line shows the saturation profile of water from the model developed. This demonstrates the solution of two-phase flow equations. The dotted line shows the saturation profile as computed from the analytical solution of Buckley Leverette equation (Figure 1). The solution of two phase flow equation is in good agreement with the solution of the Buckley Leverett equation. The result therefore validates the model.

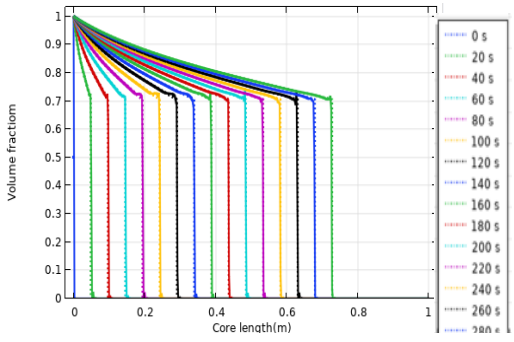

Figure 1: Solution of two-phase flow equation in a porous medium (solid lines) and analytical solution of the Buckley Leverette equation (dotted lines)

3.2 Results of the Model Performance on Water Flooding Process

The result for water flooding simulation is as shown in Figures 2. From the result, there is a formation of water front that displaces the oil which can be removed at the production end of the core. The oil is completely removed from the core after three hours of water saturation.

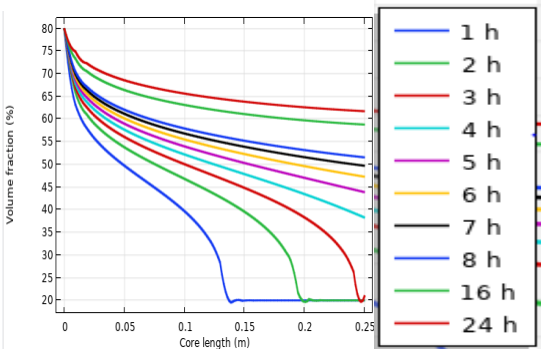

Figure 2: Water saturation profile for water flooding

The oil recovery model to investigate the amount of oil produced during water flooding was upgraded. This result could be compared to the work of Diaz-Viera and Ortiz-Tapia (2015) (Figure 3(a) and (b)). The point graphs represent the percentage of oil recovery during water flooding. In both cases, about 74% recovery was observed. In the model, oil recovery was related to time, but in real life processes, oil recovery is usually related to injected pore volume. The relationships as represented in Equations 34 and 35 was applied and the results are as shown in Figure 4.

$$IPV = \frac{tu}{V_p} \tag{34}$$

$$V_p = \phi V_B \tag{35}$$

where IPV is the injected pore volume, t is the time, u is the flow rate, V_p is the pore volume, ϕ is the porosity and V_B is the bulk volume.

Licensed Under Creative Commons Attribution CC BY

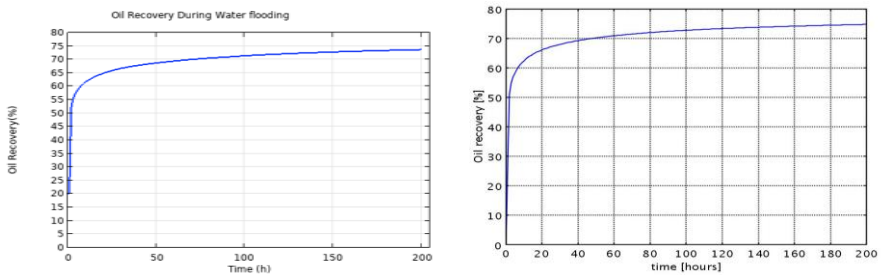

(a) (b)

Figure 3: Oil production curve from (a) the model and (b) previous work of Diaz-Viera and Ortiz-Tapia (2015)

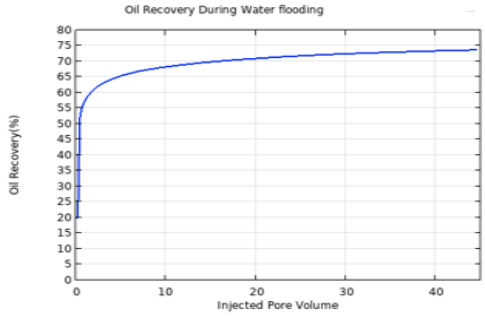

Figure 4: Oil Recovery against Injected Pore Volume

3.3 Result of Experimental EOR Process Simulation

The oil production model developed was applied to replicate a real life experimental work. This was shown from the experimental result of controlled salinity EOR as carried out by Udoh and Vinogradov (2021). The result of the model could be compared with the result of the experimental work. In the experimental work, there was a switch from the flow rate of 1ml/min to 3ml/min during the flooding process but the model did not accommodate that. The flow rate in the model was fixed.

The results of the model at the flow rate of 1ml/min and 3ml/min using the data of CSB obtained from the experimental work are as shown in Figures 5(a) and (b). The experimental result is as shown in Figure 5(c). The result simulation, at 3ml/min could be compared with the experimental result as shown in Figure 5(d). Oil recovery in the experimental and the simulation work using the model was observed to be about 77%.

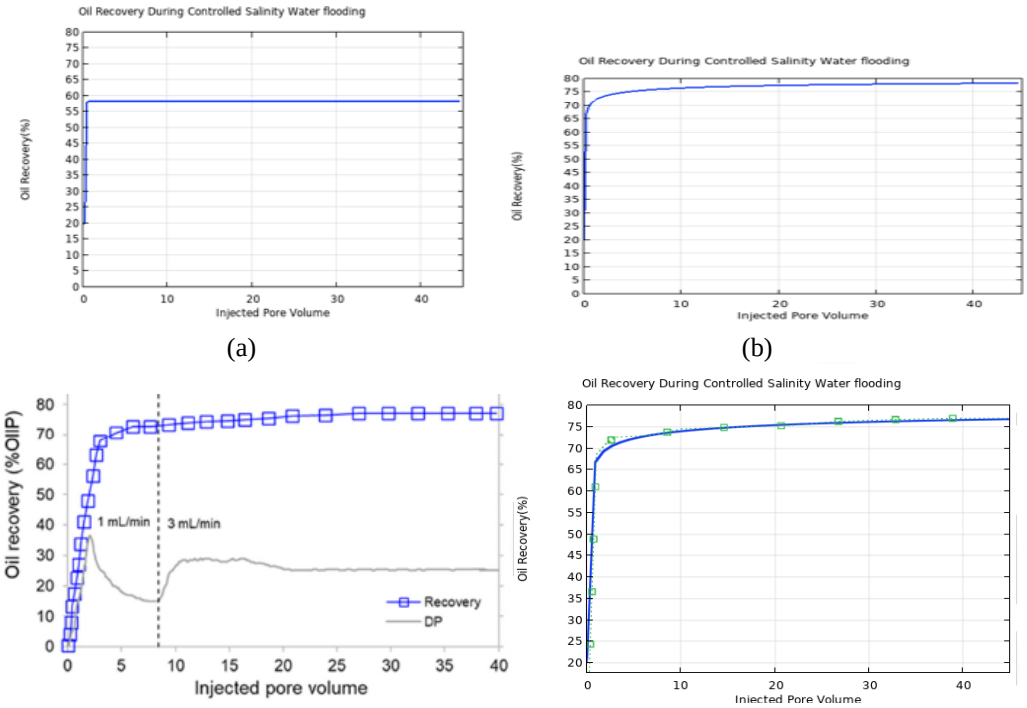

(a) (b)

(c) (d)

Figure 5: (a) Oil recovery during simulation of CSB injection at 1ml/min (b) Oil recovery during simulation of CSB injection at 3ml/min (c) Experimental result of CSB injection (d) Simulation result (solid blue line) and experimental result (dotted green line with squares) of CSB injection at 3ml/min.

Licensed Under Creative Commons Attribution CC BY

Similarly, when the data of the experimental work on core flooding experiment using controlled salinity bio-surfactant brine with rhamnolipids (CSBSB-R) was used, lower oil recovery of about 61% was observed when the flow rate of 1ml/min was used (Figure 6(a)) and about 80.5% of oil recovery was observed when 3ml/min flow rate was considered (Figure 6(b). The experimental result is shown in Figure 6(c). The model result at 3ml/min also agrees with the experimental result as shown in Figure 6(d).

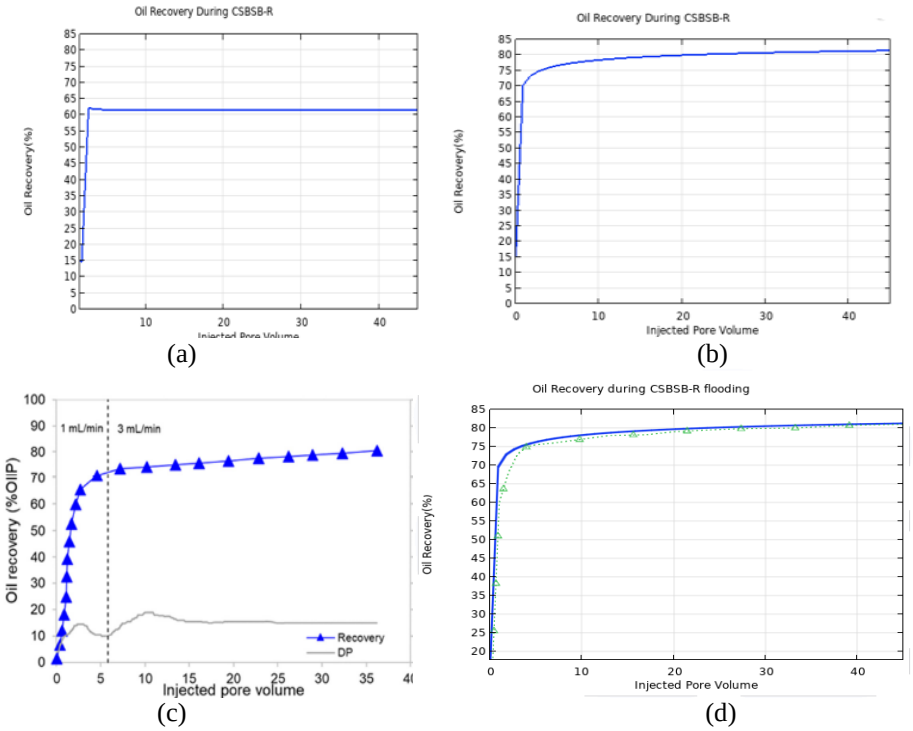

Figure 6: (a) Oil recovery during modeling of CSBSB-R injection at 1ml/min (b) Oil recovery during modeling of CSBSB-R injection at 3ml/min (c) Experimental result of CSBSB-R injection (d) Modeling result (solid blue line) and experimental result (dotted green line with triangles) of CSBSB-R injection at 3ml/min

From CSBSB-G simulation, the same data for its experimental work were used. The simulation result at 1ml/min is as shown in Figure 7(a) and about 62.5% oil recovery is observed. Higher oil recovery of about 82% was observed when the flow rate of 3ml/min was used (Figure 7(b)). Experimental result is as shown in Figure 7 (c). The simulation result at 3ml/min can also be compared with the experimental work as shown in Figure 7(d).

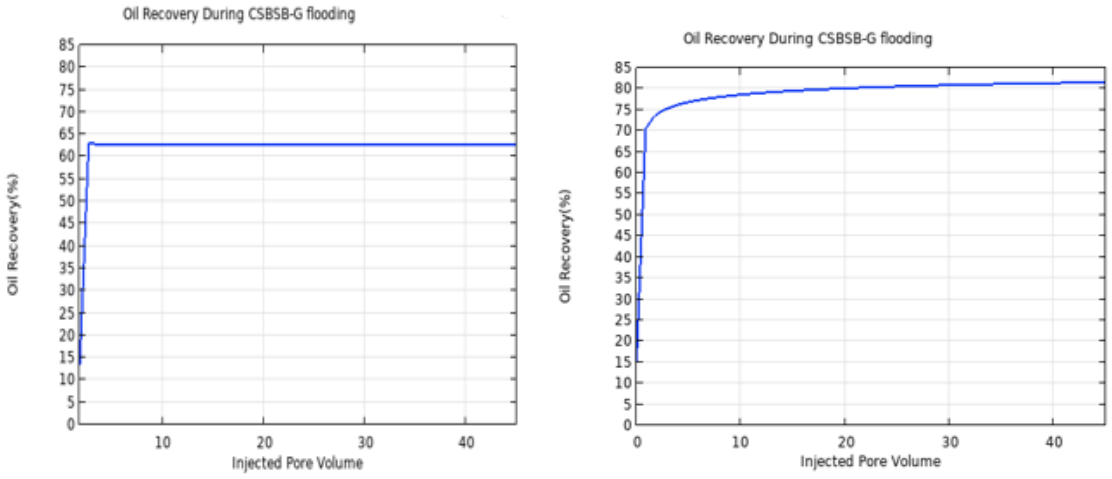

Licensed Under Creative Commons Attribution CC BY

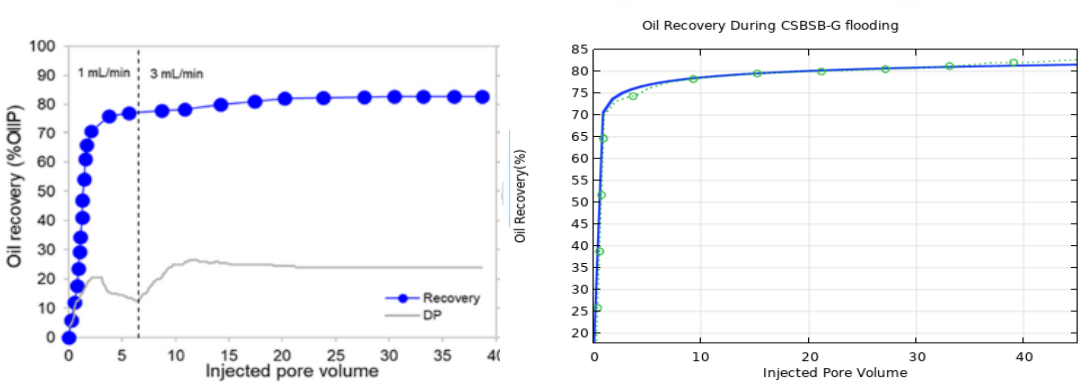

(c) (d)

Figure 7: (a) Oil recovery during simulation of CSBSB-G injection at 1ml/min (b) Oil recovery during simulation of CSBSB-G injection at 3ml/min (c) Experimental result of CSBSB-G injection (d) Simulation result (solid blue line) and experimental result (dotted green line with circles) of CSBSB-R injection at 3ml/min

From the above analysis, lower oil recoveries were observed when the simulation was done at 1ml/min injection in comparison to the experimental result at the same rate. This can be due to the limitation of the model developed. The model could not replicate the experimental work exactly. In the experimental work, there was a switch from the flow rate of 1ml/min to 3ml/min during the flooding process, but the model did not accommodate that. The flow rate in the model was fixed. However, the results of the higher flow rate of 3ml/min agree with the experimental results. The results obtained from the simulation and the experimental work at 3ml/min suggest that the model can be applied but there is a need to improve on the model to accommodate its deficiencies.

4. Conclusion

The model developed can be used to investigate controlled salinity EOR and other EOR processes. This can reduce the stress that is usually associated with laboratory experimental works.However, it can be improved to accommodate the deficiency for a better performance.

References

[1] Ahmed, T. (2006). *Reservoir Engineering Handbook*, (Third Edition). Gulf Professional Publishing, (Chapter 4).

[2] Alfazazi, U., AlAmeri, W. and Hashmet, M. R. (2019). Experimental Investigation of Polymer Flooding with Low-Salinity Preconditioning of High Temperature–High-Salinity Carbonate.Reservoir. *Journal of Petroleum Exploration and Production Technology (2019) 9:1517–1530doi.org/10.1007/s13202-018-0563-z.*

[3] Arabzai, A. and Honma, S. (2013). Numerical Simulation of the Buckley-Leverett Problem. *Proc. Schl. Eng. Tokai Univ., Ser. E 38 2013.*

[4] Diaz-Viera, M. A., Lopez-Falcon1, D. A., Moctezuma-Berthier1, A., A. and Ortiz-Tapia, A. (2008). COMSOL Implementation of a Multiphase Fluid Flow in a porous Media. *Excerpt from proceedinds of COMSOL Conference 2008 Boston*.

[5] Diaz-Viera, M. A. and Ortiz-Tapia. A. (2015). A Flow and Transport Model in Porous Media for Microbial Enhanced Oil Recovery Studies Using COMSOL Multiphysics® Software. *COMSOL Conference 2015 Boston, USA, October 7-9.*

[6] Gbadamosi, A O., Junin, R., Manan, M. A., Agi A. and Yusuff, A. S. (2019). An Overview of Chemical Enhanced Oil Recovery: Recent Advances and Prospects. *International Nano Letters (2019) 9:171–202 https://doi.org/10.1007/s40089-019-0272-8..*

[7] Keshtkar, S., Sabeti, M. and Mohammadi, M. H. (2016). Numerical Approach for Enhanced Oil Recovery with Surfactant Flooding, *Petroleum 2 (2016) 98-107.*

[8] Khusainova, A. (2016). Thesis on Enhanced Oil Recovery with Application of Enzymes; PhD Thesis. *Center for Energy Resources EngineeringDepartment of Chemical and Biochemical EngineeringTechnical University of DenmarkKongensLyngby, 2800Denmark.*

[9] Li, K., and R. N. Horne 2006. Comparison of methods to calculate relative permeability from capillary pressure in consolidated water-wet porous media. *Water Resour. Res., 42, W06405, doi:10.1029/2005WR004482*

[10] Mandal, A. (2015). Chemical enhanced oil recovery: a review. *International Journal for Oil, Gas and Coal Tecnology, Vol. 9, No. 3, pp.241-264..*

[11] Nasiri, H., Spildo, K and Skauge, A. (2009). Use of Enzymes to Improve Waterflood Performance. *Center for Integrated Petroleum Research (CIPR), Bergen, Norway, SCA 2009-28.* .

[12] Neumaier, A. 2004. Mathematical Modelling, *www.mat.univie.ac.at/neum/papers.htm#model.*

[13] Patel J., Borgohain, S., Kumar, M., Rangarajan, V., Somasundaran, P. and Sen, R. (2015). Recent developments in microbial enhanced oil recovery Renewable and Sustainable Energy. *Reviews 52 (2015) 1539–1558.*

[14] Rahayyem, M., Mostaghimi. P., Alzahid, Y.A., Halim, A., Evangelista, L. and Ryan T. (2019).

[15] Enzyme Enhanced Oil Recovery EEOR: A Microfluidics Approach, *Society of Petroleum Engineers, SPE-195116-MS, doi.org/10.2118/195116-MS.*

[16] Szymkiewicz, A. 2007. Numerical Simulation of One-Dimensional Two Phase Flowin Porous Media. Archives of Hydro-Engineering and Environmental

Licensed Under Creative Commons Attribution CC BY

Mechanics Vol. 54 (2007), No. 2, pp. 117–136 © IBW PAN, ISSN 1231–3726.

[17] Tunio, S. Q.,Tunio, A. H.,Ghirano, N. A. and El Adawy, Z. M. (2011).Comparison of Different Enhanced Oil Recovery Techniques for Better oil. *International Journal of Applied Science and Technology Vol. 1 No. 5.*

[18] Udoh, T and Vinogradov, J. (2021). Controlled Salinity-Biosurfactant Enhanced Oil Recovery at Ambient and Reservoir Temperatures—An Experimental Study. *Energies 2021, 14, 1077. https://doi.org/10.3390/en14041077.*

[19] Zhengwen Zeng, Z. (2021). Green Enzyme Enhanced Oil Recovery. *Glob J Eng Sci. 8(1): 2021. GJES.MS.ID.000676. DOI: 10.33552/GJES.2021.08.000676.*

Licensed Under Creative Commons Attribution CC BY